

An Algorithm for a Class of Direct and Inverse Scattering Problems

Raadhakrishnan Poovendran
HSTX/Dept. Of Electrical Engineering
The University of Michigan
Ann Arbor, MI 48109

John E. Dorband
NASA/Goddard Space Flight Center
Greenbelt, MD 20771

Abstract

A new, highly parallel algorithm for a class of direct and inverse scattering problems is proposed. It is also shown that this new algorithm reduces the noise propagation exhibited by the existing algorithms, and produces error terms that are proportional to the square of the discrete step size. Numerical examples are presented to illustrate the proposed algorithm.

1 Introduction

In this paper, we propose a new, highly parallel algorithm for solving a class of 1-D direct and inverse scattering problems in time domain via an invariant imbedding approach.

Direct or inverse scattering problems arise in several interesting physical processes such as speech processing, geophysics, acoustics, transmission line modeling, etc. The direct or forward problem is to construct the reflection coefficients of the medium by probing the medium with the input signal and measuring the output or response of the medium. The inverse problem is to reconstruct the medium properties from the knowledge of a segment of the reflection coefficients.

The most popular and recent algorithms used to solve these scattering problems are dynamic deconvolution and differential methods in time or frequency domain. These algorithms assume that the medium is inhomogeneous but sufficiently smooth. This assumption enables one to view the medium as a physical system consisting of multiple layers, across which the medium properties vary in a smooth, inhomogeneous manner. The inverse problem deals with the material reconstruction in a thin differential layer, whereas the direct problem deals with the construction of the reflection kernel differentially.

The new algorithm presented in this paper is a highly decoupled reformulation of the existing in-

variant imbedding algorithms, using the assumptions made in the original formulation. The proposed reformulation leads to the complete decoupling of the reflection coefficients in a layer. As a result, the noise introduced due to computational error of a point in a layer does not affect another entry of the reflection kernel in the same layer. Moreover, by choosing perturbed initial conditions for the forward and inverse problems it is shown that the new formulation, unlike the conventional algorithm [1], is quite robust for small signal to noise ratios.

Section 2 starts with a review of the invariant imbedding formulation, including a discussion of the shortcomings of the conventional algorithms. Then, the necessary modifications leading to a highly decoupled and readily parallelizable algorithm are described. Section 3 includes numerical examples to validate the proposed method.

2 Invariant Imbedding Formulation

This section describes the formulation of the direct and inverse invariant imbedding problems in terms of the material properties and the reflection kernel of the layered medium. The first step is to formalize the idea of the reflection kernel for a thin strip of the medium. The subsequent discussion closely follows the ideas presented in [1].

To derive the mathematical relationship between the reflection kernel and the material properties of the medium, we assume the following:

1. The medium is inhomogeneous and isotropic in the interval $a_0 < z < b_0$ and homogeneous elsewhere.
2. The material properties of the inhomogeneous region of the medium are sufficiently smooth and vary as a function of the depth z of the medium.
3. The material properties for $z < a_0$ and $z > b_0$ match those at $z = a_0$ and $z = b_0$, respectively.

Hence, the incident and the reflected wavefields can be easily identified.

Fig. 1. shows the velocity profile $c(z)$ of the wavefield.

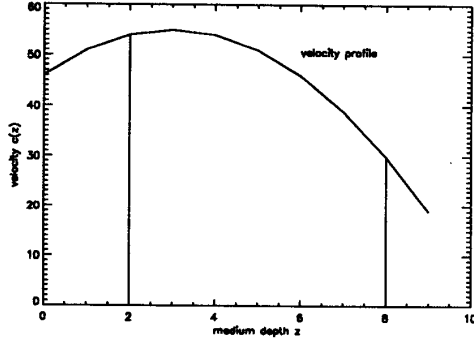


Fig. 1. Velocity profile $c(z)$ as a function of the medium depth.

The velocity $c(z)$ in the inhomogeneous region of the medium ($a_0 < z < b_0$) is continuous at the boundaries a_0 and b_0 .

In the electromagnetic case, the waves are described by the equation:

$$U_{zz} - \epsilon(z)\mu_0 U_{tt} = 0, \quad (1)$$

where U is the transverse component of the E field, $\epsilon(z)$ is the permittivity, and μ_0 is the permeability of the medium. (U_{zz} and U_{tt} represent the second order partial derivatives of the wavefield U with respect to the variables z and t , respectively.)

In the elastic wave case, the equation is:

$$(EU_z)_z - \rho U_{tt} = 0, \quad (2)$$

where U is the displacement, ρ is the density, and $E = \lambda + 2\mu$ for transverse waves and $E = \mu$ for the longitudinal waves (λ and μ are Lamé parameters).

Consider a subinterval $a < z < b$ that is imbedded in the inhomogeneous region of the medium, where the material properties for $z < a$ and $z > b$ match those at $z = a$ and $z = b$, respectively. The incident wavefield $U^i(z, t)$ can be written as:

$$U^i(z, t) = f\left(\frac{-(z-a)}{c(a)} + t\right), \quad (3)$$

where $c(a)$ is the wave speed at $z = a$ and the incident wavefield is along the $+z$ direction. The wave reflected by the inhomogeneous region $a < z < b$ propagates in the $-z$ direction and is given by:

$$U^r(z, t) = g\left(\frac{(z-a)}{c(a)} + t\right) \quad z > a; \quad t > 0, \quad (4)$$

where the functions $f(t)$ and $g(t)$ are the time records of the incident and reflected wavefields measured at $z = a$, respectively. Since the reflection process is causal and invariant under time translation, f and g must be related by an equation of the form:

$$g(t) = \int_{-\infty}^t f(t-s)R^+(a, b, s)ds, \quad (5)$$

where $R^+(a, b, s)$ is the causal reflection kernel for the subinterval $[a, b]$.

Equations (1) through (4) can be rewritten in travel time coordinates using the following transformations:

$$x = \Phi(z) = \int_{a_0}^z \frac{ds}{c(s)}, \quad u(x, t) = U(z, t),$$

$$R(x, y, t) = R^+(\Phi^{-1}(x), \Phi^{-1}(y), t). \quad (6)$$

For the electromagnetic case [4]:

$$c(z) = \{\mu\epsilon(z)\}^{\frac{1}{2}}, \quad A(x) = -\frac{\partial}{\partial x} \log(c(z)); \quad (7)$$

and for the elastic case [4]:

$$c(z) = \sqrt{\frac{E}{\rho}}, \quad A(x) = \frac{\partial}{\partial x} \log(\rho c(z)). \quad (8)$$

Given $0 < x < y$ and $t > 0$, the following equation results:

$$\begin{aligned} \frac{\partial}{\partial x} R(x, y, t) - 2 \frac{\partial}{\partial t} R(x, y, t) = \\ - \frac{A(x)}{2} R(x, y, t) \otimes R(x, y, t), \end{aligned} \quad (9)$$

where \otimes denotes the linear convolution over the variable x .

The boundary conditions for the causal operator $R(x, y, t)$ are given by:

$$R(x, y, 0^+) = -\frac{A(x)}{4}; \quad R(y, y, t) = 0. \quad (10)$$

From equation (9) we note the following:

1. The system represented by (9) can be used to solve either the direct or the inverse scattering problems.
2. In the direct problem we are given $A(x)$ for $0 < x < \Phi(b_0)$, and using equation (9) we can solve for the reflection kernel of the medium, $R(0, \Phi(b_0), t) = R^+(a_0, b_0, t)$.

3. In an inverse problem, we are given a finite initial section of the reflection kernel $R^+(a_0, b_0, t)$ for $0 < t < 2\Phi(b_0)$. ($2\Phi(b_0)$ is the round trip travel time for a pulse to go to the depth b_0 and return to the surface). From the knowledge of this data, $A(x)$ is reconstructed for $0 < x < \Phi(b_0)$. This computation is carried out over the triangular grid defined by $0 < x < \Phi(b_0)$ and $0 < t < 2\Phi(b_0)$. An efficient way of solving the inversion problem is to use equation (10) to obtain $A(x)$ at the given depth x , and then compute $R(x + \delta x, y, t)$ by advancing one layer into the medium using equation (9).

4. The reflection process is causal and the reflection kernel is a causal operator. Moreover, the inhomogeneous region of the medium is assumed to have material properties that are time invariant. Hence, the reflection kernel is a causal time invariant operator.

2.1 Computational Algorithms

This subsection deals with the conventional invariant imbedding algorithms and their shortcomings.

Assuming that the travel time coordinates are normalized to unity, we set $y = 1$ and represent $R(x, y, t)$ as $R(x, t)$. Furthermore, we set the computational grid for the problem to be $0 < x < 1$ and $0 < t < 2(1 - x)$. For the forward problem $A(x)$ is known and $R(0, t)$ has to be computed for $0 < t < 2$. For the inverse problem $R(0, t)$ is specified for $0 < t < 2$ and $A(x)$ has to be obtained for $0 < x < 1$.

Using the Trapezoidal rule, equation (9) can be rewritten as:

$$\begin{aligned}
 &R(x_0 + \epsilon, t - 2(x_0 + \epsilon)) - R(x_0, t - 2x_0) = \\
 &-\frac{\epsilon}{4}[A(x_0 + \epsilon)R \otimes R(x_0 + \epsilon, t - 2(x_0 + \epsilon)) \\
 &+ A(x_0)R \otimes R(x_0, t - 2x_0)]. \quad (11)
 \end{aligned}$$

The discrete version of equation (11) can be derived by noting that the total round trip time of the wave is twice the time taken for it to reach depth x in travel time coordinates. Hence, the computation is done on a triangle defined by the straight lines $x = 0$, $t = 0$ and $t = 2(1 - x)$ as shown in Fig. 2.

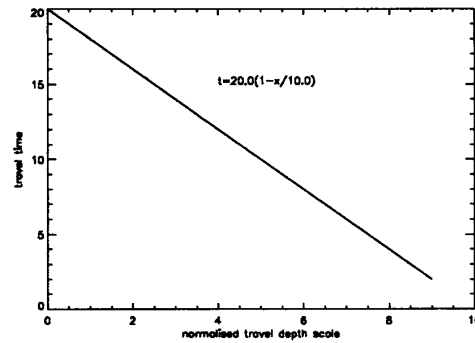


Fig. 2. Computational grid in travel time coordinates.

A computational scheme based on the trapezoidal rule can be derived for $R_{i,j}$ where index i represents the layer number and the index j represents the location or the pointer to an entry of the reflection kernel for a given layer. Computational grid for the forward and the reverse problems are shown in Fig. 3(a) and Fig. 3(b), respectively.

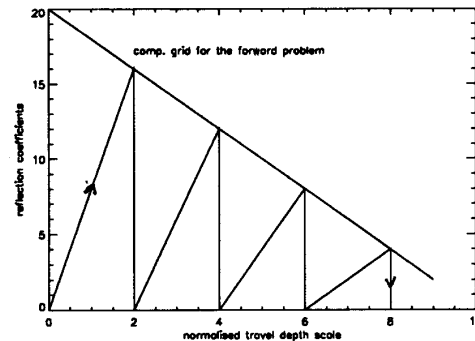


Fig. 3(a). Conventional computational grid for the forward scattering.

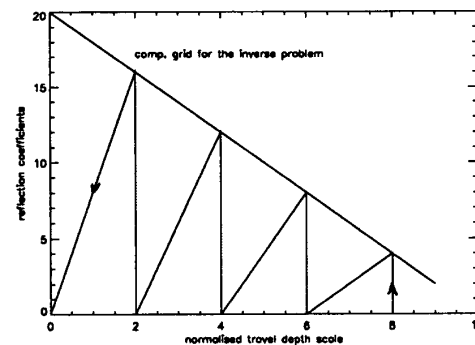


Fig. 3(b). Conventional computational grid for the inverse scattering.

The direction of the arrow in each figure indicates the direction in which the computation proceeds. For example in figure 3(a), if we run the forward algorithm and want to compute a given entry R_{i_0, j_0} , we need to know all the points in layers $i > i_0$ and $j < j_0$. A similar statement holds for the inverse problem with the reversal of the inequalities. Hence, the existing formulation is highly coupled and computationally intensive even in a parallel computer. Moreover, any computational noise added in an intermediate level will affect every point computed thereafter.

2.2 Reformulation of the Computational Algorithm

In this subsection we show that the algorithms proposed by Coronas[1] can be modified to derive faster and more efficient algorithms, comparable to the Schur formulations. We show that the new formulation does not require any information about the entries in the same layer to compute a given point $R_{i,j}$. For example, in order to run the forward algorithm and compute the point $R_{i,j}$, the reformulation does not require any knowledge about the remaining points in the i^{th} layer. This leads to a readily parallelizable and highly decoupled algorithm. One additional advantage of the new formulation is that any noise added in an intermediate step will affect only a selected set of points computed afterwards.

Since the medium is assumed to be sufficiently smooth, the reflection kernel is a smooth function and hence a continuous function of the depth x . For example, the reflection kernel $R(x_0 + \frac{\epsilon}{2}, t - 2(x_0 + \frac{\epsilon}{2}))$ is left and right continuous. This leads to the following constraint:

$$\begin{aligned} \lim_{\epsilon \rightarrow 0} \frac{1}{\epsilon} \{ R(x_0 + \frac{\epsilon}{2}, t - 2(x_0 + \frac{\epsilon}{2})) - R(x_0, t - 2x_0) \} = \\ \lim_{\epsilon \rightarrow 0} \frac{1}{\epsilon} \{ R(x_0 + \epsilon, t - 2(x_0 + \epsilon)) - R(x_0 + \frac{\epsilon}{2}, t - 2(x_0 + \frac{\epsilon}{2})) \}. \end{aligned} \quad (12)$$

In the computational algorithm described in the previous subsection, ϵ denotes the discrete step size. Since the reflection kernel is a smooth function of depth, instead of integrating over the interval $(x_0, x_0 + \epsilon)$, we can integrate over the interval $(x_0, x_0 + \frac{\epsilon}{2})$ and $(x_0 + \frac{\epsilon}{2}, x_0 + \epsilon)$. Using the results from equation (12), the following forward equation can be derived:

$$\begin{aligned} R_{i,j-1} - R_{i-1,j} = \\ -\frac{\epsilon^2}{2} \left[\frac{A(i+1)}{2} \sum_{k=1}^{j-1} R_{i+1,k} R_{i+1,j-1-k} \right. \end{aligned}$$

$$\left. + \frac{A(i)}{2} \sum_{k=1}^j R_{i,k} R_{i,j-k} \right]. \quad (13)$$

Clearly, the reflection kernel has to be computed for the $(i-1)^{\text{st}}$ layer, and index j is bounded above by $(n-i-1)$ instead of the conventional bound $n-i$.

Similarly, using the equation (12) the discrete version of the inverse problem can be derived as:

$$\begin{aligned} R_{i,j-1} - R_{i-1,j} = \\ -\frac{\epsilon^2}{2} \left[\frac{A(i+1)}{2} \sum_{k=1}^{j-1} R_{i+1,k} R_{i+1,j-1-k} \right. \\ \left. + \frac{A(i)}{2} \sum_{k=1}^j R_{i,k} R_{i,j-k} \right]. \end{aligned} \quad (14)$$

The modified computational grids for the forward and the inverse problems are shown in Fig. 4 and Fig. 5 respectively.

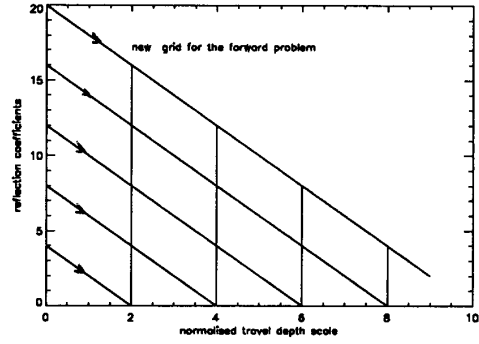


Fig. 4(a). Modified computational grid for the forward problem.

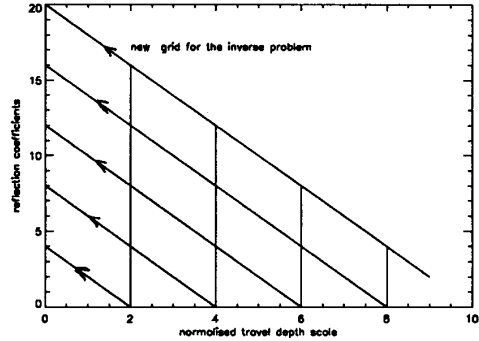


Fig. 4(b). Modified computational grid for the inverse problem.

Equations (13) and (14) are not only highly decoupled but also lead to the same order of accuracy as the existing algorithms [1]. This claim is theoretically validated in the next subsection.

2.3 Error Analysis of the New Algorithm

Since the material properties of the medium are sufficiently smooth, the Taylor series can be used to represent the reflection kernel in terms of the variable x . The Taylor series representation of $R(x_0 + \frac{\epsilon}{2}, t - 2(x_0 + \frac{\epsilon}{2}))$ with respect to the point $R(x_0, t - 2x_0)$ results in the following equation:

$$R(x_0 + \frac{\epsilon}{2}, t - 2(x_0 + \frac{\epsilon}{2})) = \sum_{k=0}^{\infty} \frac{(\frac{\epsilon}{2})^k}{k!} \frac{\partial^k}{\partial x^k} R(x_0, t - 2x_0). \quad (15)$$

Similarly, the Taylor series expansion of $R(x_0 + \frac{\epsilon}{2}, t - 2(x_0 + \frac{\epsilon}{2}))$ with respect to the point $R(x_0 + \epsilon, t - 2(x_0 + \epsilon))$ results in the following equation:

$$R(x_0 + \frac{\epsilon}{2}, t - 2(x_0 + \frac{\epsilon}{2})) = \sum_{k=0}^{\infty} (-1)^k \frac{(\frac{\epsilon}{2})^k}{k!} \frac{\partial^k}{\partial x^k} R(x_0 + \epsilon, t - 2(x_0 + \epsilon)). \quad (16)$$

After rearranging terms, the following equation can be derived for the forward problem:

$$R(x_0 + \frac{\epsilon}{2}, t - 2(x_0 + \frac{\epsilon}{2})) - R(x_0, t - 2x_0) = \frac{1}{2} \{ [R(x_0 + \epsilon, t - 2(x_0 + \epsilon)) - R(x_0, t - 2x_0)] \} + \frac{\epsilon^2}{4} \{ [A(x_0 + \epsilon) \frac{\partial}{\partial x} R \otimes R(x_0 + \epsilon, t - 2(x_0 + \epsilon))] \} + O(\epsilon^3) + \dots \quad (17)$$

Equation (17) shows that the forward algorithm produces error terms of the order ϵ^2 , where ϵ is the discrete step size of the algorithm. Hence, by properly choosing the value of the step size, computational error can be made as small as necessary. Clearly, error will be strictly zero for the linear trajectory of R . It can be shown that the inverse algorithm also produces a similar error equation with $(-\epsilon)$ substituting (ϵ) .

3 Numerical Results

In this section we describe the numerical simulations performed using the reformulated invariant imbedding algorithm.

Simulations were aimed at testing the following issues:

1. To check the validity of the reformulation for the sequential version given a fixed discretization.

2. To implement a completely parallel algorithm for the forward and inverse problems.
3. To compare the computational timings for variable layer numbers for the sequential and parallel algorithms.

The following initializations were made in the computation:

1. The input of the medium was assumed to be $A(x) = \sin(4\Pi \frac{x}{n+1}) + 2$, where n represented the number of layers and the discrete step size ϵ was set equal to $\frac{1}{n}$.
2. For the forward problem, $A(i)$ was assumed to be known for $i = 0$ to $i = n$. The reflection kernel of the medium was constructed differentially using equation (9) (Details available in [5]).
3. For the inverse problem, values of $R(0, j)$ for $j = 0$ to $j = n$ were assumed to be known. Equations (9) and (1) were used to reconstruct the medium properties in a differential manner.

The following details the computational steps involved in

- (a) Forward Problem: (Computation of the reflection coefficients)

- i. Initialization

$$R(0, 0) = -A(0)/4;$$

- ii. Do Parallel : For $i = 1 : n, j = 1 : n - i$

$$R_{i,j-1} - R_{i-1,j} =$$

$$-\frac{\epsilon^2}{2} \left[\frac{A(i+1)}{2} \sum_{k=1}^{j-1} R_{i+1,k} R_{i+1,j-1-k} \right.$$

$$\left. + \frac{A(i)}{2} \sum_{k=1}^j R_{i,k} R_{i,j-k} \right]$$

$$R(i, 0) = -A(i)/4;$$

- (b) Inverse Problem: (Computation of the inhomogeneous region of the medium from the knowledge of the impulse response)

- i. Initialization

$$A(n) = -4R(n, 0);$$

- ii.

- Do Parallel: For $i = 1 : n, j = 1 : n - i - 1$

$$R_{i+2,j-1} - R_{i+1,j} =$$

$$-\frac{\epsilon^2}{2} \left[\frac{A(i+1)}{2} \sum_{k=1}^{j-1} R_{i+1,k} R_{i+1,j-1-k} \right.$$

$$+ \frac{A(i)}{2} \sum_{k=1}^j R_{i,k} R_{i,j-k}]$$

$$A(i) = -4R(i, 0).$$

Numerical computations were carried out using the new algorithm in the sequential and the parallel versions. Algorithms were implemented using MPL C for the MASPAC super computer.

Fig.5 shows the input and output waveforms.

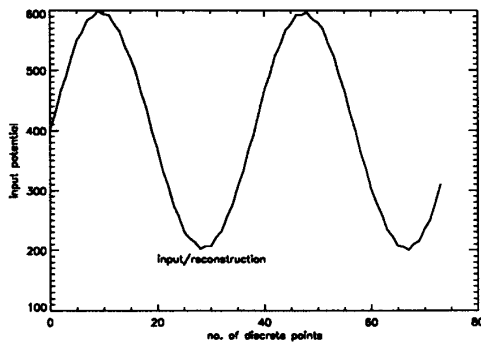


Fig. 5. Input and Reconstructed waveforms. These waveforms are identical to the machine precision.

As claimed earlier, these two waveforms are indistinguishable. Fig. 6 shows the computational timings for the reformulated sequential and the parallel implementations.

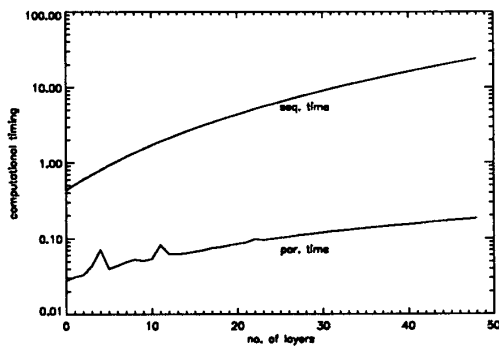


Fig. 6. Computational timings of the sequential and the parallel algorithms.

Fig.7 shows the ratios of the timings in the log scale.

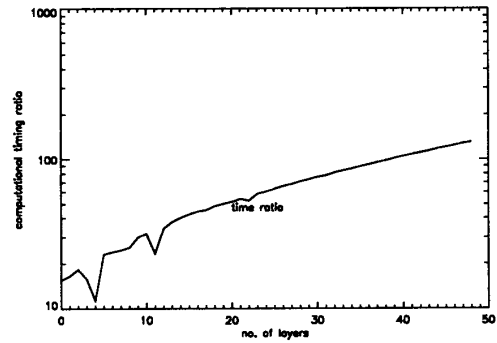


Fig. 7. Ratios of the computational timings in log scale. The graph shows asymptotically linear gain.

4 Conclusion

In this paper, we presented an efficient reformulation of a class of 1-D direct and inverse scattering problems, employing invariant imbedding methods. Unlike the conventional algorithms [1], the new formulation decouples the reflection kernel in a given layer.

It was shown that the smoothness assumptions made in the formulation of the original problems were sufficient for the reformulation. Moreover, these assumptions also led to efficient initialization schemes for the inverse problem.

The error in the reformulation was shown to be controlled by the step size (varied as the square of the step size). Due to its decoupling nature, the new formulation completely eliminated any error propagation between any two points in the same layer. This simply was not the case with the conventional algorithms.

Though we assumed the inhomogeneous region of the medium to be sufficiently smooth, the numerical simulations showed that the differential form captures the sharp discontinuities very well. In fact the input and the reconstructed potential waveforms were identical up to six decimal places as shown in Fig. 6. Numerical comparisons validated the theoretical derivations.

References

- [1] J.P. Coronas, M.E. Davison, and R.J. Krugger, "Wave splittings, invariant imbedding and inverse scattering," *Inverse Optics, Proc. SPIE 419*, edited by Anthony J. Devaney (SPIE, Bellingham, WA, 1983), pp. 102-106.

- [2] J.P. Corones, M.E. Davison, and R.J. Krugger, "The effect of dissipation in one-dimensional inverse problems," *Inverse Optics, Proc. SPIE 413*, edited by Anthony J. Devaney (SPIE, Bellingham, WA, 1983), pp. 107-114.
- [3] J.P. Corones, M.E. Davison, and R.J. Krugger, "Direct and inverse scattering in the time domain via invariant imbedding equations," *J.Acoust.Soc.Am.* 74(5), Nov, 1983, pp. 1535-1541.
- [4] Andrew E. Yagle and Benard C. Levy, "Application of Schur algorithm to the inverse problem for a layered acoustic medium", *J.Acoust.Soc.Am.* 76(1). July, 1984, pp. 301-308.
- [5] Raadhakrishnan Poovendran, "A new parallel algorithm for a class of direct and inverse Scattering Problems," *Internal quarterly report, USRA*, July-Sept. 1991.
- [6] Alfred M. Bruckstein, Benard C. Levy and Thomas Kailath, "Differential methods in inverse scattering," *SIAM J.APPL. MATH*, vol. 45, 2, April, 1985, pp. 312-335.